

1 **RESEARCH ARTICLE**

2
3 **Pod indehiscence in common bean is associated to the fine regulation of**
4 ***PvMYB26* and a non-functional abscission layer**

5 **Valerio Di Vittori^a, Elena Bitocchi^a, Monica Rodriguez^{b,c}, Saleh Alseekh^{d,e}, Elisa Bellucci^a,**
6 **Laura Nanni^a, Tania Gioia^f, Stefania Marzario^f, Giuseppina Logozzo^f, Marzia Rossato^g,**
7 **Concetta De Quattro^g, Maria L. Murgia^b, Juan José Ferreira^h, Ana Campa^h, Chunming**
8 **Xuⁱ, Fabio Fiorani^j, Arun Sampathkumar^d, Anja Fröhlich^d, Giovanna Attene^{b,c}, Massimo**
9 **Delledonne^g, Björn Usadel^j, Alisdair R. Fernie^{d,e}, Domenico Rau^b, Roberto Papa^{a,k}.**

10

11 ^a Dipartimento di Scienze Agrarie, Alimentari e Ambientali, Università Politecnica delle Marche,
12 via Brecce Bianche, 60131, Ancona, Italy

13 ^b Dipartimento di Agraria, Università degli Studi di Sassari, Via E. De Nicola, 07100 Sassari,
14 Italy

15 ^c Centro per la Conservazione e Valorizzazione della Biodiversità Vegetale, Università degli
16 Studi di Sassari, SS 127bis, km 28.500 Surigheddu, 07041 Alghero, Italy

17 ^d Max-Planck-Institute of Molecular Plant Physiology, Am Muehlenberg 1, Potsdam-Golm,
18 14476 Germany

19 ^e Center of Plant Systems Biology and Biotechnology, 4000 Plovdiv, Bulgaria

20 ^f Scuola di Scienze Agrarie, Forestali, Alimentari ed Ambientali, Università degli Studi della
21 Basilicata, viale dell'Ateneo Lucano 10, 85100 Potenza, Italy

22 ^g Dipartimento di Biotecnologie, Università degli Studi di Verona, Cà Vignal 1, Strada Le Grazie
23 15, 37134 Verona, Italy

24 ^h Plant Genetics Group, Agri-Food Research and Development Regional Service (SERIDA),
25 33300, Asturias, Spain

26 ⁱ Key Laboratory of Molecular Epigenetics of the Ministry of Education (MOE), Northeast
27 Normal University, Changchun, 130024 China

28 ^j Institute of Biosciences and Geosciences (IBG-2): Plant Sciences, Forschungszentrum Jülich
29 GmbH, 52425 Jülich, Germany

30 ^kCorresponding author: Roberto Papa (r.papa@univpm.it)

31

32 **Short title:** The pod-shattering syndrome in common bean

33

34 **One-sentence summary:** A non-functional abscission layer determines the loss of pod
35 shattering; mapping data, and parallel gene expression and histological analysis support
36 *PvMYB26* as the candidate gene for pod indehiscence.

37

38 The author responsible for distribution of materials integral to the findings presented in this
39 article in accordance with the policy described in the Instructions for Authors
40 (www.plantcell.org) is: Roberto Papa (r.papa@univpm.it).

41

42

43

44 **ABSTRACT**

45 In legumes, pod shattering occurs when mature pods dehisce along the sutures, and detachment
46 of the valves promotes seed dispersal. In *Phaseolus vulgaris*, the major locus *qPD5.1-Pv* for pod
47 indehiscence was identified recently. We developed a BC4/F4 introgression line population and
48 narrowed the major locus down to a 22.5-kb region. Here, gene expression and a parallel
49 histological analysis of dehiscent and indehiscent pods identified an *AtMYB26* orthologue as the
50 best candidate for loss of pod shattering, on a genomic region ~11 kb downstream of the highest
51 associated peak. Based on mapping and expression data, we propose early and fine up-regulation
52 of *PvMYB26* in dehiscent pods. Detailed histological analysis establishes that pod indehiscence is
53 associated to the lack of a functional abscission layer in the ventral sheath, and that the key
54 anatomical modifications associated with pod shattering in common bean occur early during pod
55 development. We finally propose that loss of pod shattering in legumes resulted from histological
56 convergent evolution and that this is the result of selection at orthologous loci.

57

58

59 **Keywords:** pod shattering, common bean, *MYB26*, genome-wide association study, gene
60 expression, pod anatomy, convergent evolution, introgression lines.

61

62 INTRODUCTION

63

64 Loss of seed shattering is a paradigmatic example of the changes that have occurred to crop plant
65 traits compared to their wild progenitors, which collectively constitute the ‘domestication
66 syndrome’ (Hammer 1984). In wild species, specialised seed-dispersal strategies are of
67 fundamental importance for plant survival and fitness. Conversely, in domesticated forms, loss or
68 reduction of seed shattering is desired to reduce yield losses.

69 Due to its complex evolutionary history, common bean (*Phaseolus vulgaris* L.) is an
70 excellent model to study the domestication process (Bitocchi *et al.*, 2017), which included its
71 parallel domestication in the Andes and Mesoamerica (Bitocchi *et al.*, 2013). In *P. vulgaris*, the
72 dry beans are characterised by different degrees of pod shattering. These represent the majority of
73 the domesticated pool (Gepts and Debouck 1991), where a limited level of pod shattering has
74 been conserved to favour the threshing of the dry pods. Variations in the pod shattering intensity
75 are also associated with the environmental conditions during maturation (e.g., humidity and
76 temperature) (Parker *et al.*, 2020).

77 Secondary domestication events have resulted in the development of totally indehiscent
78 snap-bean cultivars, with a dominance of the Andean gene pool among commercial snap beans
79 (Wallace *et al.*, 2018). Snap beans are suitable for green pod production due to the low fibre
80 content in the pod walls and sutures (i.e., the stringless type). Pioneering investigations into
81 *Arabidopsis thaliana* have reconstructed the genetic pathways associated with its fruit
82 differentiation and silique shattering, which provides a model of the mechanisms underlying seed
83 dispersal for other crop species (for review, see Di Vittori *et al.*, 2019). In common bean,
84 Koinange *et al.* (1996) identified the qualitative locus *St* on chromosome Pv02 for the presence of
85 pod suture string. Their observation that pod fibre content correlates with pod shattering was
86 confirmed by Murgia *et al.* (2017), who identified an association between the carbon and lignin
87 contents and modulation of pod shattering. Nanni *et al.* (2011) and Gioia *et al.* (2013) identified
88 the orthologous genes of *AtSHP* (Liljegren *et al.*, 2000) and *AtIND* (Liljegren *et al.*, 2004),
89 respectively, in common bean, where *AtIND* was co-mapped with *St* (Koinange *et al.*, 1996).
90 However, *PvSHP* and *PvIND* did not show any polymorphic sequences associated with
91 occurrence of pod shattering (Nanni *et al.*, 2011, Gioia *et al.*, 2013). Recently, Rau *et al.* (2019)
92 identified a major locus on chromosome Pv05 for pod indehiscence (*qPD5.1-Pv*), which was also

93 confirmed by Parker *et al.* (2020). Rau *et al.* (2019) thus proposed a model in which at least three
94 additional hypostatic loci on chromosomes Pv04, Pv05 and Pv09 are involved in modulation of
95 pod shattering, with multifactorial inheritance of the trait previously suggested by Lamprecht
96 (1932). The recent identification of a major locus for pod shattering in common bean (Rau *et al.*,
97 2019) and in cowpea (Lo *et al.*, 2018) in a syntenic region on chromosome Pv05 supports the
98 occurrence of convergent molecular evolution in legume species. Moreover, Parker *et al.* (2020)
99 suggested that the gene orthologous to *GmPDHI* in soybean (Funatsuki *et al.*, 2014) is also
100 involved in the modulation of pod shattering in common bean.

101 In the present study, we developed a population of 1,197 BC4/F4 introgression lines (ILs)
102 dedicated to pod shattering syndrome traits, with the aim to narrow down the major locus
103 *qPD5.1-Pv*, and to promote recombination at QTLs for pod shattering. We also performed
104 differential expression analysis at the transcriptome level (i.e., RNA-seq) between wild and
105 domesticated pods, and at the major locus *qPD5.1-Pv* for target genes (i.e., qRT-PCR), using a
106 comparison of indehiscent and highly dehiscent pods from near isogenic lines. The expression
107 analysis for the putative structural genes of lignin biosynthesis and a parallel histological analysis
108 of the indehiscent and dehiscent pods allow reconstruction of the main phenotypic events
109 associated to the modulation of pod shattering, that occur early during pod development. Finally,
110 through identification of orthologous genes, expression-analysis and selection signatures, we
111 propose several candidate genes with potential roles in the modulation of pod shattering, both at
112 the genome-wide level and at known QTLs.

113

114

115 **RESULTS**

116

117 **Histological modifications underlying pod shattering in common bean**

118 Lignification of the ventral and dorsal sheaths starts at 6 days after pod setting (DAP) for the
119 pods of both the totally indehiscent variety Midas (Figure 1A, B; Supplemental Figure 1A, B)
120 and the highly shattering IL 244A/1A (Figure 1C, D; Supplemental Figure 1C, D).

121 Higher lignification was seen here for both the ventral (Figure 1C, D) and the dorsal
122 (Supplemental Figure 1C, D) sheaths of the highly shattering IL 244A/1A, compared to the
123 corresponding tissues of the indehiscent genotype Midas (Figure 1A, B, Supplemental Figure 1A,
124 B). Moreover, a different conformation of the ventral sheath was seen comparing these non-
125 shattering and high-shattering pods. For 10-day-old pods (i.e., at 10 DAP), the lignification
126 pattern of the ventral suture clearly differed between the totally indehiscent variety (Figure 2A,
127 B) and the highly dehiscent recombinant inbred line (RIL) MG38 (Figure 2C, D) and IL
128 244A/1A (Figure 2E, F).

129 A few layers of cells were lignified in the abscission zone of the non-shattering type
130 (Figure 2B), compared to the equivalent tissue of the highly shattering lines (Figure 2D, F),
131 which lacked lignification. This modification is potentially involved in prevention of pod
132 opening. The walls of the cells that surrounded the abscission zone in the ventral sheath were
133 heavily thickened in the highly shattering pods (Figure 2D, F), compared to the equivalent cells
134 of the totally indehiscent pods (Figure 2B). This might increase the mechanical tension within the
135 ventral suture, to thus promote pod shattering. Moreover, at 10 DAP, the highly shattering pods
136 showed an internal lignified valve layer (Supplemental Figure 2B, C), which was not seen for the
137 indehiscent pods of the variety Midas (Supplemental Figure 2A). At 14 DAP, the degree of
138 lignification of the ventral suture, and both the ventral sheath and the abscission zone
139 conformations strongly differed between the indehiscent variety Midas (Supplemental Figure 3A,
140 B) and the highly shattering RIL MG38 (Supplemental Figure 3C, D) and IL 244A/1A
141 (Supplemental Figure 3E, F). The histological conformation of mature pods at 30 DAP is
142 presented in Figure 3.

143 In the region where the pods open at maturity (i.e., the abscission zone), in the highly
144 shattering type, there were five layers of cells that completely lacked lignification of the cell

145 walls (Figure 3D), compared to the lignification of the equivalent cells for the totally indehiscent
146 pods (Figure 3B). We therefore suggest that the non-functional abscission layer is responsible for
147 the loss of pod shattering in common bean. The cell walls were heavily thickened in the ventral
148 sheath of the high-shattering pods (Figure 3D), compared to those of the ventral sheath of the
149 indehiscent pods (Figure 3B). The lumen of the cells also appeared to be almost occluded in
150 some of the cells of the high-shattering pod sheaths. Interestingly, there were a few layers of
151 lignified, but not heavily thickened, cells across the ventral sheath of the mature dehiscent pods
152 (Figure 3C, D, dashed ellipses). It is possible that different degrees of wall thickening along the
153 sutures is required to create the mechanical tension needed for pod shattering and/or pod twisting.
154

155 **Segregation of pod shattering**

156 Phenotyping for pod shattering on 100 lines from six BC4/F1 families revealed uniformity in F1
157 for the presence of pod shattering. Phenotyping of a subset of 509 BC4/F2 lines, from the first
158 planting and that uniformly reached the maturation, identified 386 and 120 dehiscent and
159 indehiscent plants, which fits the 3:1 expected ratio of a Mendelian trait ($\chi^2 = 0.45$)
160 (Supplemental Table 1). The expected segregation ratio of a Mendelian trait was also observed
161 when each of the BC4/F2 subpopulations were analysed separately (Supplemental Table 2), and
162 for a subset of lines from the BC4/F3 population that produced enough pods for a reliable post-
163 harvest phenotyping of pod shattering (356 putative dehiscent vs 193 putative indehiscent lines)
164 ($\chi^2 = 1.28$) (Supplemental Table 3). Moreover, 354 BC4/F2 dehiscent ILs showed pod twisting to
165 different degrees (classed as: 1% to <10%; $\geq 10\%$ to <24%; $\geq 24\%$; Supplemental Table 1), while
166 32 dehiscent lines did not show any twisting; assuming the action of duplicated and independent
167 genes with cumulative effects, this fits to a 15:1 twisting/ non-twisting ratio ($\chi^2 = 2.74$).

168 Due to the high correlation that was observed here between the field and post-harvest
169 phenotyping of the BC4/F2 population ($r = 0.81$; $p = 7.33 * 10^{-118}$), the post-harvest evaluation
170 was also integrated into the subsequent analysis. In all, 1,197 BC4/F4 ILs were phenotyped for
171 pod shattering in the field and/or after harvesting. When the field and post-harvest phenotypes
172 were combined (i.e., defined as the ‘SH y/n’ [pod shattering, yes/no] trait), 940, 11 and 243 ILs
173 were classified as dehiscent, intermediate and indehiscent, respectively (Supplemental Table 4).
174 Overall, 721 F3 families were represented at the beginning of the BC4/F4 field experiment (i.e.,
175 2,230 BC/F4 seeds were sown from 721 F3 plants), from which 502 F3 families produced

176 BC4/F4 progenies. Of these, and as expected, 95 indehiscent F3 lines gave complete indehiscent
177 F4 progeny, while segregation was still observed within 55 F3 families.

178

179 **Genome-wide association study for pod shattering and fine mapping of the major locus**

180 ***qPD5.1-Pv***

181 A genome-wide association study (GWAS) for pod shattering was performed using a dataset of
182 19,420 single-nucleotide polymorphisms (SNPs) from genotype-by-sequencing (GBS) analysis,
183 which were identified across 1,196 BC4/F4 ILs (Supplemental Figure 4). GWAS for the trait
184 defined as ‘SH y/n’ (dehiscent vs indehiscent lines) identified a major locus for occurrence of pod
185 shattering at the end of chromosome 5 (*qPD5.1-Pv*) (Figure 4); here, 52 SNPs showed
186 association ($-\log_{10}p > 6$) with the presence/ absence of pod shattering in the interval between the
187 S5_38322754 and S5_39384267 markers.

188 The major locus *qPD5.1-Pv* was also in the association for the following mapping
189 analyses: when 18 ILs for which the phenotype score was not clearly assigned were removed (see
190 Supplemental Table 4) (Supplemental Figure 5A); when the ‘SH y/n’ trait that included plants
191 with an intermediate phenotype was used (Supplemental Figure 5B); when the presence/ absence
192 of pod shattering was only from the field phenotyping (Supplemental Figure 5C); when the post-
193 harvest phenotype was used (putative dehiscent vs putative indehiscent lines; Supplemental
194 Figure 5D); when all of the phenotypic classes from the post-harvest evaluation were used
195 (quantitative score; Supplemental Figure 5E); and when the percentage of twisting pods per plant
196 was used (field evaluation; Supplemental Figure 5F). These GWAS data are summarised in the
197 Supplemental Table 5, while Supplemental Figure 6 shows the expanded major QTL for all of
198 these mapping strategies. A few recurrent highly associated SNPs were identified within the
199 major locus (Figure 4; Supplemental Figure 6; and Supplemental Table 5). These identified three
200 genomic regions around 38.61 Mb, 38.79 Mb and 39.12 Mb on chromosome Pv05. In particular,
201 S5_38611412 was among the best associated SNPs for all of the mappings, with a few
202 surrounding SNPs with high p values (Supplemental Table 5; Supplemental Figure 6). After
203 narrowing the QTL to a 22.5 kb surrounding region (from S5_38605293 to S5_38627793), a few
204 candidates were identified, among which there was a protein kinase (Phvul.005G157300), a
205 phospholipid-transporting ATPase (Phvul.005G157400; with the highest associated SNP

206 S5_38611412) and a nucleotidase (Phvul.005G157500). The main peak was located ~11 kb
207 before a MYB26 transcription factor (Phvul.005G157600), the orthologue that is involved in
208 anther dehiscence and secondary cell-wall differentiation in *A. thaliana* (Yang *et al.*, 2007).
209 Moreover, a cluster of lipoxygenase genes were located on a tightly associated genomic region,
210 from ~48 kb to ~17 kb upstream of the main peak (Phvul.005G156700, Phvul.005G156800,
211 Phvul.005G156900, Phvul.005G157000).

212

213 **Identification of candidate genes for pod shattering and gene-expression analysis**

214 The candidate genes were identified based on the annotation, the function of orthologues in
215 legume species and *A. thaliana*, the differential expression analysis using RNA-seq data between
216 wild and domesticated pods, the differential expression at the target candidate genes for the major
217 locus *qPD5.1-Pv* (qRT-PCR) in a comparison of near isogenic lines, and the evidence of
218 selection signatures from Schmutz *et al.* (2014) and Bellucci *et al.* (2014).

219

220 *Candidate genes at the major locus qPD5.1-Pv*

221 Supplemental Data Set 1 summarises the genes within the major locus *qPD5.1-Pv*, along with
222 their differential expression and selection signatures. Overall, *qPD5.1-Pv* contains 128 genes, of
223 which 29 were differentially expressed (from RNA-seq data), and 15 were under selection in the
224 Mesoamerican gene pool, according to Schmutz *et al.* (2014) and/or Bellucci *et al.* (2014). Four
225 genes were both differentially expressed and under selection.

226 Located ~11 kb downstream to the most significant peak, Phvul.005G157600 is
227 orthologous to *AtMYB26* (Yang *et al.*, 2007). Phvul.005G157600 expression was up-regulated in
228 5-day-old dehiscent pods (i.e., Midas vs G12873), and down-regulated in G12873 dehiscent pods
229 at 10 DAP (Supplemental Data Set 1; row 50). Down-regulation of *PvMYB26* expression was
230 also seen for the comparison of Mesoamerican domesticated and wild (MD vs MW) at 5 DAP.
231 Moreover, two genes located downstream to *PvMYB26* (Phvul.005G157700, Phvul.005G157800)
232 on the physical map showed signatures of selection.

233 Within the highest associated region to which *qPD5.1-Pv* was narrowed down
234 (S5_38605293:S5_38627793), Phvul.005G157400 and Phvul.005G157500 did not show
235 differential expression or selection signatures, while no reads were mapped (i.e., RNA-seq) on

236 Phvul.005G157300 in any of the samples (Supplemental Data Set 1; rows 47-49). In addition,
237 *qPD5.1-Pv* contained a cluster of three differentially expressed linoleate 9S-lipoxygenase genes
238 (Phvul.005G156700, Phvul.005G156900, Phvul.005G157000; Supplemental Data Set 1; rows 41,
239 43, 44) that were located upstream (from ~48 to ~17 kb) of the highest associated peak for pod
240 indehiscence. In more detail: Phvul.005G156700 was down-regulated for Midas *versus* G12873
241 and Andean domesticated snap bean (AD_Snap) *versus* Andean wild (AW) at 10 DAP;
242 Phvul.005G156900 expression was up-regulated for Midas *versus* G12873 at 10 DAP; while
243 Phvul.005G157000 was down-regulated for the totally indehiscent pods (Midas *vs* G12873) at 10
244 DAP, and also showed signatures of selection in the Mesoamerican gene pool. In the region that
245 surrounds SNP S5_39120955, which was also highly associated to occurrence of pod shattering
246 (see Supplemental Table 5), there was a cluster of leucine-rich repeat (LRR) coding genes. In
247 particular, Phvul.005G163800 and Phvul.005G163901 (Supplemental Data Set 1; rows 108,
248 110), which are both annotated as LRR-protein-kinase related, show differential expression for
249 AD_Snap *versus* AD, AD *versus* AW, and MD *versus* MW at 5 DAP (Phvul.005G163800), and
250 for Midas *versus* G12873 at 10 DAP (Phvul.005G163901). SNP S5_38792327 was also one of
251 the best associated SNPs at the major locus *qPD5.1-Pv* (see Supplemental Table 5), and it was
252 located within a fatty acid omega-hydroxy dehydrogenase (Phvul.005G159400; Supplemental
253 Data Set 1; row 69), which, however, did not show selection signatures or significant differential
254 expression. Finally, Phvul.005G164800 showed higher expression in indehiscent pods of Midas
255 at 5 DAP and 10 DAP, compared to G12873 (Supplemental Data Set 1; row 119), and it was
256 annotated as ZINC FINGER FYVE-DOMAIN-CONTAINING PROTEIN.

257

258 *Candidate genes with a putative function in pod shattering based on their orthologues*

259 Orthologous genes in common bean that in other species have pivotal roles in modulation of pod
260 shattering, cell-wall modifications and putative pod-shattering-related functions were identified.
261 These orthologous genes are reported in Supplemental Data Set 2, along with the results of the
262 differential expression analysis (i.e., RNA-seq) and the signatures of selection.

263 First, we consider as promising candidates the orthologous genes located close to the
264 known QTLs for pod shattering. On chromosome Pv02, Phvul.002G271000 (*PvIND*; [Gioia *et*
265 *al.*, 2013]) is orthologous to *AtIND* (Liljegren *et al.*, 2004), and it was highly expressed in the
266 snap-bean group compared to AW at 10 DAP (Supplemental Data Set 2; row 28); moreover,

267 close to *PvIND*, we identified the NAC transcription factor Phvul.002G271700 (orthologous to
268 NAC082). Both Phvul.002G271000 and Phvul.002G271700 map to the *St* locus (Koinange *et al.*,
269 1996). On chromosome Pv03, Phvul.003G252100 is orthologous to *Glycine max PDH1*
270 (Funatsuki *et al.*, 2014), which was recently proposed as a candidate for modulation of pod
271 shattering in common bean (Parker *et al.*, 2020); here, Phvul.003G252100 was up-regulated for
272 Midas *versus* G12873 at 5 DAP and 10 DAP, and down-regulated for AD *versus* AW at 5 DAP,
273 and MD *versus* MW at 10 DAP, with a signature of selection in the Andean gene pool
274 (Supplemental Data Set 2; row 45). On chromosome Pv04, Phvul.004G144900 is orthologous to
275 the MYB52 transcription factor, which maps to a region associated with modulation of pod
276 shattering (Rau *et al.*, 2019); here, Phvul.004G144900 was less expressed for AD_Snap *versus*
277 AW and MD *versus* MW, both at 10 DAP (Supplemental Data Set 2; row 50). Moreover, ~660
278 kb downstream, Phvul.004G150600 is a PIN family member, and thus putatively involved in
279 correct regulation of auxin efflux. Phvul.004G150600 showed higher expression for indehiscent
280 pods (Midas *vs* G12873) at 5 DAP, with a signature of selection (Supplemental Data Set; row
281 51). On chromosome Pv09, close to the significant SNP for shattering modulation at ~30 Mb that
282 was identified by Rau *et al.* (2019), and within the QTL identified also by Parker *et al.* (2020),
283 Phvul.009G203400 is the orthologous to *AtFUL* (Gu *et al.*, 1998); interestingly,
284 Phvul.009G203400 shows parallel selection between the gene pools (Schmutz *et al.*, 2014), and
285 congruently across different studies (Schmutz *et al.*, 2014 and Bellucci *et al.*, 2014)
286 (Supplemental Data Set 2; row 93). In the same region, two physically close genes,
287 Phvul.009G205100 and Phvul.009G205200, are orthologous to *Cesa7*, and they showed selection
288 signatures. Moreover, Phvul.009G205100 was less expressed in the domesticated pods
289 (Supplemental Data Set 2; rows 94, 95).

290 Here, we also identified potential candidates at the genome-wide level based on their
291 orthology with genes with well-described functions in the modulation of seed dispersal and/or
292 fruit development in other species, and because they showed signatures of selection and/or
293 interesting differential expression patterns. Those that can be highlighted are:
294 Phvul.002G294800, as orthologous to *GmPDH1*; Phvul.003G166100 and Phvul.011G100300, as
295 putative orthologous to *Sh1*; Phvul.003G182700 and Phvul.003G281000, as orthologous to
296 *AtFUL*; Phvul.007G100500, as putative orthologous to *Shattering4*; Phvul.008G114300 and
297 Phvul.010G011900, as orthologous to *Replumless*, *SH5* and *qSH1*; and in particular,

298 Phvul.010G118700, as orthologous to *NST1* and *GmSHAT1-5* (Supplemental Data Set 2). These
299 data suggest that these genes might share a conserved pod-shattering-related function. Moreover,
300 an *AtMYB26* orthologue on chromosome Pv10, Phvul.010G137500, was under-expressed in the
301 AD and AD_Snap pods, compared to the wild pods at 5 DAP, while it was more highly
302 expressed for MD *versus* MW at 10 DAP (Supplemental Data Set 2; row 100).

303

304 *Structural genes in the phenylpropanoid biosynthesis pathway*

305 In all, 109 genes were identified as putatively involved in the pathway of lignin biosynthesis
306 based on gene annotation and orthologous relationships with genes from *G. max* and *A. thaliana*
307 (Supplemental Data Set 3). No putative structural genes were identified within *qPD5.1-Pv*;
308 however, several genes for lignin biosynthesis were located close to the major locus
309 (Supplemental Figure 7). According to the RNA-seq expression data here, 50 (46%) of the total
310 109 structural genes were significantly differentially expressed for Midas *versus* G12873, for at
311 least one of the two developmental stages that were considered ($p < 0.01$; with 41 of these at p
312 < 0.001) (Supplemental Data Set 3). This suggests that the developmental phase between 5 DAP
313 and 10 DAP is of particular importance for pod lignin biosynthesis.

314

315 *Expression patterns (qRT-PCR) of target candidates within the major locus qPD5.1-Pv*

316 The expression pattern for *PvMYB26* (Phvul.005G157600) was investigated in the pods of the
317 totally indehiscent variety Midas, as well as for the three near isogenic ILs 038B/2A2, 244A/1A
318 and 232B across eight pod developmental stages, using qRT-PCR. Up to the 4 DAP stage, no
319 differential expression was seen between the mean expression of the three highly shattering lines
320 and the totally indehiscent Midas (Figure 5).

321 *PvMYB26* (Phvul.005G157600) was up-regulated at 5 DAP and 7 DAP in the dehiscent
322 pods (fold-change, 2.20, 2.62, respectively; Supplemental Table 6), although at 7 DAP, only the
323 expression of IL 232B was significantly different from Midas (Supplemental Figure 8). At 9
324 DAP, and with greater differences seen also at 11 DAP, *PvMYB26* was more highly expressed in
325 the indehiscent pods of the variety Midas, as compared to the dehiscent lines, both as their
326 combined mean expression (Figure 5) and as their individual expression (Supplemental Figure 8;
327 and Supplemental Table 6). Reassuringly, the expression patterns for *PvMYB26*

328 (Phvul.005G157600) were in agreement between the RNA-seq data (Midas vs G12873,
329 Supplemental Data Set 1; row 50) and the qRT-PCR data. Among the target candidates for the
330 major locus, efficient amplification was obtained for: Phvul.005G156900 (linoleate 9S-
331 lipoyxygenase); Phvul.005G161600 (translation initiation factor 2 subunit 3); Phvul.005G161800
332 (rRNA [uracil(747)-C(5)]-methyltransferase); Phvul.005G161900 (BHLH87 transcription factor
333 similar to *AtIND*); Phvul.005G163901 (LEUCINE-RICH REPEAT PROTEIN KINASE-
334 RELATED); Phvul.005G164800 (ZINC FINGER FYVE DOMAIN CONTAINING PROTEIN);
335 Phvul.005G165600 (auxin-responsive protein IAA18-related); Phvul.005G165900 (LYSM
336 domain receptor-like kinase); and Phvul.005G166300 (Myb-like DNA-binding domain).
337 Phvul.005G161900 showed overall lower expression across the pod developmental stages and
338 plant genotypes (for both qRT-PCR and RNA-seq) when compared to the other target candidates.
339 However, slightly, but significantly, increased expression was seen for the dehiscent pods at 5
340 DAP (Supplemental Table 6).

341 As mentioned above, Phvul.005G156900 is a promising target candidate due to its
342 genomic position and expression pattern (i.e., RNA-seq data). However, differential expression
343 was observed only at 7 DAP for each of the dehiscent lines individually, but with variable
344 expression patterns across the three dehiscent lines (Supplemental Table 6). Phvul.005G161800
345 showed higher expression in the dehiscent pods across all of the pod stages, with the greatest
346 fold-change (3.273) seen for 11 DAP (Supplemental Table 6). These qRT-PCR data suggest that
347 Phvul.005G161800 has a shattering-related function. The LRR-protein kinase related gene
348 Phvul.005G163901 was highly expressed in the dehiscent pods with the most consistent
349 differences seen at 4 DAP and 13 DAP (Supplemental Table 6). However, its expression pattern
350 differed to that for the RNA-seq data (Midas vs G12873, Supplemental Data Set 1; row 110).
351 This can potentially be explained by its expression being modulated after the expression of other
352 genes involved in pod shattering, and its function is indeed worth further investigation.

353 When the shattering lines were considered as a combined group, Phvul.005G165900
354 showed lower expression in the highly shattering pods at 9 DAP, 11 DAP and 13 DAP
355 (Supplemental Table 6). Moreover, the Phvul.005G165900 expression pattern was in agreement
356 with the RNA-seq expression data (Midas vs G12873 at 10 DAP; see Supplemental Data Set 1;
357 row 130).

358 Overall, the best target candidate genes for *qPD5.1-Pv* are summarised in Supplemental
359 Table 7.

360

361

362

363 **DISCUSSION**

364 Our results confirm that pod indehiscence in snap beans is controlled by a Mendelian locus with
365 recessive inheritance. Here, we narrowed the major QTL *qPD5.1-Pv* down to a 22.5-kb genomic
366 region that is located ~11 kb upstream of *PvMYB26*. Among the candidate genes for loss of pod
367 shattering, *PvMYB26* is the best candidate because of its specific differential expression pattern
368 between dehiscent and indehiscent pods, which is in agreement with the histological
369 modifications associated to pod shattering across the same pod developmental phases. Moreover,
370 the histological modifications are coherent with the function of *AtMYB26* in *A. thaliana*. Here,
371 we also provide a list of candidate genes potentially involved in pod-shattering-related functions,
372 through orthologue identification, selection signatures, and differential gene expression between
373 wild and domesticated pods (i.e., RNA-seq) and/or between near isogenic lines (i.e., qRT-PCR).

374 We also demonstrate that pod indehiscence is associated with a lack of a functional
375 abscission layer in the ventral sheath, due to ectopic lignification of a few layers of cells. Also,
376 the key phenotypic events associated with pod shattering arise early in pod development, between
377 6 DAP and 10 DAP.

378

379 **Phenotypic architecture of pod shattering**

380 Here, we propose that the failure of the formation of the abscission layer due to ectopic
381 lignification is associated with pod indehiscence. This is similar to the ‘welding’ mechanisms
382 previously defined for soybean by Dong *et al.* (2014), and more recently reported by Takahashi *et*
383 *al.* (2019a) in an EMS mutant of *Vigna stipulacea*. Moreover, the cell-wall thickening pattern that
384 we observed in the cells surrounding the abscission zone of the pods is in agreement to previous
385 studies on *A. thaliana*, where in the wild-type, lignification at the valve margin close to the
386 abscission layer is required for silique shattering (Liljegren *et al.*, 2004). Interestingly, valve
387 margin lignification is also associated with pod coiling in *Medicago truncatula* (Fourquin *et al.*,
388 2013). We have also confirmed that an internal lignified valve layer forms in highly dehiscent
389 pods, compared to indehiscent pods, which occurs early, before 10 DAP (Murgia *et al.*, 2017).
390 This phenotype is most likely associated to the modulation of pod twisting, which from the
391 phenotypic segregation analysis here, appears to be regulated in shattering pods by the action of
392 at least two independent loci. Lignin deposition in the sclerenchyma of pod valves that is

393 mediated by *GmPDH1* is also required for dehiscence modulation in soybean (Funatsuki *et al.*,
394 2014). This parallelism further reinforces the occurrence of convergent phenotypic evolution at
395 the histological level between common bean and soybean for loss and reduction of pod
396 shattering. Similarly, in some Brassicaceae, such as *Cardamine hirsuta*, asymmetric lignin
397 deposition in *endocarp b* of the silique valves also ensures explosive seed dispersal and silique
398 coiling (Hofhuis *et al.*, 2016). Furthermore, we propose that the key histological modifications
399 associated to pod shattering occur between 6 DAP and 10 DAP. This agrees with the observation
400 that 46% of the putative structural genes of lignin biosynthesis are differentially expressed in the
401 same phase comparing indehiscent and highly shattering pods.

402

403 ***PvMYB26*: the best candidate for the major locus *qPD5.1-Pv***

404 Among the candidate genes that we investigated, we propose *PvMYB26* as the best candidate at
405 the major locus for pod indehiscence. This is based on its genomic location, and on the parallel
406 analysis of its expression patterns between dehiscent and indehiscent pods and of the histological
407 modifications associated to pod shattering in the early phase of pod development. A role for
408 *PvMYB26* in the loss of pod shattering is strongly supported also by the function of its orthologue
409 in *A. thaliana*. Indeed, *AtMYB26* is required to establish which cells undergo cell-wall thickening
410 to promote anther dehiscence (Yang *et al.*, 2007 and 2017), and it acts upstream of the *NST1* and
411 *NST2* genes, which have key roles in silique shattering (Mitsuda and Ohme-Takagi 2008).
412 Interestingly, Takahashi *et al.* (2019b) suggested that pod shattering and pod tenderness are
413 associated to MYB26 orthologues in azuki bean (*Vigna angularis*) and cowpea (*Vigna*
414 *unguiculata*). The parallel identification of the MYB26 orthologue as the best candidate gene in
415 *P. vulgaris* and other legumes (Takahashi *et al.*, 2019b), in addition to previous data from Rau *et*
416 *al.* (2019) and Lo *et al.* (2018) in common bean and cowpea, respectively, further reinforce the
417 hypothesis of the occurrence of molecular convergent evolution for domestication of pod
418 shattering.

419 In addition to *PvMYB26*, we identified other genes that are worth highlighting. A cluster
420 of four lipoxygenase genes were identified here, and their orthologues in *A. thaliana*
421 (AT1G55020, AT3G22400) are putatively involved in defence responses, jasmonic acid
422 biosynthesis, and responses to abscisic and jasmonic acid (The Arabidopsis Information Resource
423 [TAIR] database). We also highlight Phvul.005G163901 and Phvul.005G163800 within a cluster

424 of LRR genes, and Phvul.005G161800 (rRNA [uracil(747)-C(5)]-methyltransferase).
425 Interestingly, a potential role for LRR-RLK genes in shattering-related functions, such as
426 secondary cell-wall biosynthesis and abscission processes, can be postulated according to Jinn *et*
427 *al.* (2000), Bryan *et al.* (2011), Van Der Does *et al.* (2017) and Xu *et al.* (2008).

428 Overall, no putative structural genes for lignin fell within *qPD5.1-Pv*. We suggest that
429 selection might preferentially act on regulation factors instead of genes with a central role in the
430 lignin biosynthetic pathway, perturbations of which can result in side-effects on genotype fitness
431 and/or can be disabling for normal development of the plant. However, there was a cluster of
432 putative structural genes for lignin biosynthesis close to *qPD5.1-Pv*, which suggests that they are
433 directly involved in the same pathway of the genes responsible for the major QTL.

434 Based on the evidence we present here, *PvMYB26* is the best candidate for the major
435 locus. Nevertheless, the presence of further candidates that are also organised within a cluster of
436 genes suggests that the main QTL operates in an ‘operon’-like manner. Indeed, the clustering of
437 duplicated or non-orthologous genes might provide advantages in terms of coordination of
438 expression between physically close genes that are involved in the same pathway, as for
439 secondary metabolite biosynthesis (Osbourn 2010 and Boycheva *et al.*, 2014).

440

441 ***Convergent evolution and conservation of the molecular pathway for modulation of pod*** 442 ***shattering***

443 In the present study, we identified orthologous genes that are putatively involved in pod-
444 shattering-related functions, and we analysed their expression profiles and selection signatures to
445 provide potential candidates at known QTLs and/or at the genome-wide level. Among these, we
446 highlight Phvul.002G271000 (*PvIND*), as orthologous to *AtIND* (Liljegren *et al.*, 2004), which
447 has a pivotal role in silique shattering in *A. thaliana*. Moreover, our expression data and selection
448 signatures reinforce the orthologue of *PDHI* (Funatsuki *et al.*, 2014) (*PvPdh1*;
449 Phvul.003G252100) as a strong candidate for modulation of pod shattering also in common bean
450 (Parker *et al.*, 2020). This might further suggest the occurrence of selection at orthologous loci
451 for loss or reduction of pod shattering between closely related legume species. In addition,
452 Phvul.009G203400 is a promising target candidate that shows parallel selection across the
453 Andean and Mesoamerican gene pools, according to both Schmutz *et al.* (2014) and Bellucci *et*

454 *al.* (2014). Moreover, Phvul.009G203400 is the orthologous to *AtFUL* (Gu *et al.*, 1998) which is
455 involved in valve differentiation in *A. thaliana*. Here, we also identified Phvul.010G118700, as
456 orthologous to *NST1* (Mitsuda and Ohme-Takagi 2008) and *GmSHAT1-5* (Dong *et al.*, 2014),
457 which have crucial roles in silique shattering and in pod shattering resistance in *A. thaliana* and
458 soybean, respectively. In addition to the major candidate *PvMYB26*, we also identified several
459 MYB-like protein-coding genes close to known QTLs or at the genome-wide level (see
460 Supplemental Data Set 2), and among these, a paralogue to *PvMYB26* on chromosome Pv10. The
461 function of MYB transcription factors in the regulation of both secondary cell-wall biosynthesis
462 and the phenylpropanoid pathway has been widely reported (Zhong *et al.*, 2008, Zhang *et al.*,
463 2018). Overall, the expression patterns between the wild and domesticated pods, and the presence
464 of selection signatures at orthologous genes at the genome-wide level (see Supplemental Data Set
465 2), suggest that several of these have preserved shattering-related functions, and that there has
466 been conservation across distant taxa of the pathway associated to seed dispersal mechanisms.
467 This was previously demonstrated in rice (Konishi *et al.*, 2006, Yoon *et al.*, 2014), soybean
468 (Dong *et al.*, 2014) and tomato (Vrebalov *et al.*, 2009).

469
470 Identification of the molecular and phenotypic bases of a key trait of domestication in common
471 bean such as pod shattering represents a fundamental step in the dissecting out of the
472 evolutionary history of the species. On this basis, we proposed here *PvMYB26* at the major locus
473 that controls pod indehiscence, and we have illustrated the key histological changes at the pod
474 level that are associated with pod shattering. We also used a strategy that combined expression
475 analysis, signature selection and orthologous identification, which allowed us to identify a
476 number of potential target candidate genes that need to be validated in future studies. We believe
477 that the increasing number of studies on the architecture of pod shattering will allow
478 reconstruction of the evolutionary trajectories that have led to convergent modifications across
479 legumes with ever greater resolution. With this perspective, and based on the data we have
480 presented here, we propose that loss and reduction of pod shattering might arise after selection at
481 orthologous loci, and that this has resulted in convergent evolution also at the histological level.

482

483

484 **Materials and Methods**

485

486 ***Development of the IL population***

487 Here, we developed an IL population (1,197 BC4/F4) for the mapping of pod shattering traits
488 (see Supplemental Figure 9). The IL population was developed starting from a cross between the
489 domesticated Andean variety Midas, as ‘stringless’ and totally indehiscent, and the highly
490 shattering wild Mesoamerican genotype G12873, to provide an initial set of RILs (Koinange *et al.*,
491 1996). One RIL (i.e., MG38) showed high shattering, wild traits of the seeds and pods, a
492 determinate growth habit, and the absence of photoperiod sensitivity, so it was selected as a
493 donor parent for pod-shattering traits for backcrossing with the recurrent Midas (BC1). Overall,
494 three backcrosses were performed using Midas as the recurrent parent and maintaining the
495 phenotypic selection for high shattering for each backcrossed generation, which provided 70 ILs
496 from BC3/F4:F5 families, and 217 ILs from BC3/F6:F7 families (Murgia *et al.*, 2017, Rau *et al.*,
497 2019). In the present study, six highly shattering ILs were selected as the donor parents for high
498 pod shattering, and were further backcrossed (BC4) with Midas, providing six subpopulations
499 (BC4/F1 families), for the lines: 232B (from a BC3/F4:F5 family); and 244A/1A, 038B/2A2,
500 038B/2C1, 038A/2D1 and 038B/2B1 (from BC3/F6:F7 families). Seeds of BC4/F1 individuals
501 and of the seven parental lines were pre-germinated in Petri dishes using deionised water. The
502 plants were individually grown in the greenhouse of the *Dipartimento di Scienze Agrarie,*
503 *Alimentari ed Ambientali* at the Polytechnic University of Marche in Ancona, Italy, between
504 January and May 2016. BC4/F2 seeds were collected from 100 BC4/F1 lines, and 1,353 BC4/F2
505 harvested seeds were planted in open field at Villa D’Agri, Marsicovetere (Potenza, Italy), in the
506 summer of 2016. Some of these (636 BC4/F2 seeds) were pre-germinated using vermiculite and
507 deionised water, and the seedlings were transplanted on the first planting (7 June 2016), while the
508 other 717 BC4/F2 seeds were directly sown as a second planting (26 July 2016). The pods were
509 collected from 942 BC4/F2:F3 ILs in October 2016. The BC4/F3 plants were obtained by single
510 seed descent and grown in the greenhouse between February and May 2017. With the aim to
511 reach an initial population size of 1,000 BC4/F3 individuals, two BC4/F3 seeds were sown from
512 a few dehiscent BC4/F2 lines. The pods were collected from 724 BC4/F3 individuals. Then 2,230
513 BC4/F4 seeds and 109 seeds from the seven parental lines of the new population were sown in an

514 open field at Villa D'Agri in the summer of 2017. The seeds were directly sown on 22nd June,
515 and additional sowing was performed to any recover missing plants. One BC4/F4 seed from each
516 BC4/F3 indehiscent line, and at least four BC4/F4 seeds from each BC4/F3 dehiscent line were
517 sown, with the aim to promote segregation and recombination at the major locus *qPD5.1-Pv* for
518 pod indehiscence on Pv05 (Rau *et al.*, 2019), at which a recessive domesticated allele determines
519 the totally indehiscent phenotype only in the homozygous condition. The pods were collected
520 from 1,197 BC4/F4:F5 ILs. The BC4/F2 experimental field scheme provided 12 rows, with
521 sowing distance of 0.6 m and 1.5 m within and between the rows, respectively. The BC4/F4 field
522 scheme consisted of 2,339 holes across 9 rows, with sowing distance of 0.25 m and 1.2 m within
523 and between the rows, respectively. In the field trials, the ILs were completely randomised within
524 the six BC4/F1 families. Weed control was provided using a mulching plastic sheet, and pest
525 control treatments were with Ridomil Gold (fungicide) and Klartan 20 Ew (against aphids). The
526 plants were watered daily using an automatic irrigation system, and fertilisation with nitrogen,
527 phosphorous and potassium was applied before tillage.

528

529 *Phenotyping of the IL population*

530 Phenotyping for pod shattering was performed in the field trials both qualitatively (i.e.,
531 occurrence of pod shattering, with each plant classified as dehiscent if it showed at least one
532 shattered pod), and quantitatively, by assigning a score to each dehiscent line based on the pod
533 twisting: 0 (no twisted pods per plant); 1 (1% < twisted pods < 10%); 2 ($\geq 10\%$ < twisted pods <
534 24%); and 3 ($\geq 24\%$ of twisted pods). Shattering was evaluated in the BC4/F2 ILs across four
535 dates (19 September, 29 September, 13 October, 23 October) until the uniform ripening of the
536 entire plants, and in the BC4/F4 lines across two main dates (18 October, 22 October), plus two
537 additional dates (26 October, 12 November) for plants which were not fully ripened at the earlier
538 dates. Pod shattering was also evaluated post-harvest by examination of the completely dry pods.
539 For the BC4/F1 individuals, each genotype was classified as easy to thresh (i.e., pods opened
540 very easy along sutures), similar to the highly shattering parents, or as totally indehiscent, similar
541 to the domesticated parent Midas. For the other experiments, phenotyping was performed by
542 testing the resistance to opening when the ripened pods were subjected to increasing manual
543 pressure directly on the sutures, according to the scoring system in Supplemental Table 8.
544 Moreover, a comprehensive phenotypic trait for pod shattering was assigned manually to each

545 BC4/F4 line (i.e., ‘SH y/n’; presence or absence of pod dehiscence), which combined field and
546 post-harvest phenotyping. A few BC/F4 ILs were classified as intermediate when it was not
547 possible to assign an accurate phenotype to the line.

548

549 ***Genotyping and genome-wide association study for pod shattering***

550 Young leaves were collected from 1,197 BC4/F4 ILs and 55 replicates from the seven parental
551 lines that were grown during the last IL field experiment. The leaves were dried within 12 h of
552 collection using silica gel. Genomic DNA (gDNA) was extracted from the leaves using the
553 Exgene Plant SV kit (Geneall Biotechnology) and stored at -20 °C. The gDNA integrity was
554 determined on 1% agarose gels, and the DNA quality was measured using a photometer
555 (NanoPhotometer NP80; Implen) and quantified with the dsDNA assay kits (Qubit HS; Life
556 Technologies). The gDNA concentrations were adjusted to 25 ng/μL, and the genotyping was
557 performed using GBS (Elshire *et al.*, 2011) by Personal Genomics (Verona, Italy). The protocol
558 for the GBS library preparation is provided in the Supplemental Methods (GBS library
559 preparation), according to the procedure reported in Rau *et al.* 2019. The GBS libraries were
560 sequenced (HiSeqX platform; Illumina with 2x 150 bp reads mode at Macrogen Inc. [South
561 Korea]), which generated 1.5 million fragments per sample on average. The sequencing reads
562 were demultiplexed based on their barcodes. Adapters and low-quality bases in the FASTQ files
563 were removed using the Cutadapt software, version 1.8.3 (Martin 2011). The filtered reads were
564 aligned to the reference genome of *P. vulgaris* 442 version 2.0 using the BWA-mem software,
565 version 0.7.17-r1188 (Li and Durbin 2009). The resulting BAM files were realigned using the
566 GATK RealignerTargetCreator and IndelRealigner software, version 3.8.1, to remove errors.
567 Variant calling was performed for all of the samples together, using the GATK UnifiedGenotyper
568 software, version 3.8.1 (McKenna *et al.*, 2010), and the variants were filtered based on GATK
569 best practice. The raw SNP dataset (2,419,927 SNPs) was checked for quality and loci with
570 missing data >95% and with MAF < 0.05 were excluded from further analysis. Additionally,
571 filtering was performed to remove SNPs that were either missing in one parental set (i.e. MIDAS
572 or MG38), monomorphic between parents or located in SCAFFOLDS (as SCAFFOLDS resulted
573 not associated any of the investigated traits). The dataset was then imputed for missing data by
574 using beagle.5 (Browning *et al.*, 2018). A further filtering was performed after imputation to
575 remove few more sites that were monomorphic between the parents. The final data set included

576 1253 individuals (i.e. 1196 BC/F4 ILs, 55 parental lines of the BC4 population, and the
577 references Midas and MG38) and 19,420 SNPs. GWAS was performed by using the Mixed
578 Linear Model (MLM) as implemented in the rMVP package ([https://github.com/xiaolei-](https://github.com/xiaolei-lab/rMVP)
579 [lab/rMVP](https://github.com/xiaolei-lab/rMVP)). Overall, seven descriptors of pod shattering were considered for GWAS analysis
580 from the three main phenotypic dataset (i.e., Sh y/n [integration of field and post-harvest data],
581 field, and post-harvest): Sh y/n (dehiscent vs indehiscent lines), Sh y/n after filtering (18 lines
582 that showed signs of diseases and/or a low pod production were removed), Sh y/n including lines
583 with an intermediate phenotype between the dehiscent and the indehiscent, Field (presence vs
584 absence of pod shattering), Field (percentage of twisting pods per plant), Post-harvest (putative
585 dehiscent vs putative indehiscent), Post-harvest (quantitative; mapping of all the phenotypic
586 classes 0, 1, 1.5, 2, 3).

587

588 ***RNA sequencing and differential gene expression analysis***

589 The wild dehiscent Mesoamerican genotype G12873 and the fully indehiscent Andean variety
590 Midas were grown for the collection of their pods under controlled conditions in a growth
591 chamber at the Institute of Biosciences and Geosciences (IBG-2, Forschungszentrum Jülich), in
592 2014. Two plants were planted for both the G12873 and Midas genotypes. In the same
593 experiment, a total of 57 plants were grown from 43 different genotypes, as for 14 of these, two
594 replicates were available. Considering the overall number of plants, nine were AD, 18 were AW,
595 12 were MD, and 18 were MW. Moreover, three of the nine AD were snap bean types
596 (AD_Snap; totally indehiscent), while the other six were dry beans, according to the phenotypic
597 data and the available information. The list of the accessions is provided in Supplemental Data
598 Set 4. The experimental conditions were 24/20 °C day/night temperature, 70% of relative air
599 humidity, photon lux density of 400-500 $\mu\text{mol m}^{-2} \text{s}^{-1}$, and short-day photoperiod conditions
600 (10/14 h light/dark). Fertilization was provided for N-K-P and trace elements. The pods were
601 collected for each genotype at 5 DAP and 10 DAP. These were snap-frozen in liquid nitrogen
602 before storage at $-80\text{ }^{\circ}\text{C}$. After RNA extraction, the cDNA libraries were prepared according to
603 the Illumina TruSeq RNA LT protocol, and the RNA sequencing was performed with the HiSeq
604 paired-end V4/4000 125/150 cycles sequencing technology. Sequencing was performed by the
605 Genomics and Microarray Core Laboratory at the University of Colorado in Denver (USA), and
606 the raw-data quality check and alignment were performed by Sequentia Biotech (Barcelona,

607 Spain). The read quality checking was performed on the raw sequencing data using the FastQC
608 tool, and low-quality portions of the reads were removed using BBduk. The minimum length of
609 the reads after trimming was set to 35 bp, and the minimum base quality score to 25. High quality
610 reads were aligned against the *P. vulgaris* reference genome (G19833 genome v2.1;
611 <http://phytozome.jgi.doe.gov/>) using the STAR aligner software, version 2.5.0c. The reads that
612 could not be aligned against the first reference genome were mapped against the second reference
613 genome (*P. vulgaris* L., BAT93; [Vlasova *et al.*, 2016]). FeatureCounts, version 1.4.6-p5, was
614 used to calculate the gene expression values as raw read counts. Here, the raw reads data were
615 used to perform the differential gene expression analysis across the two developmental stages,
616 using the DESeq2 package (Love *et al.*, 2014) in R (R Core Team 2019). The differential gene
617 expression was calculated for each gene (as log₂ fold-changes), and the p values were adjusted
618 according to the Benjamini-Hochberg procedure (Benjamini and Hochberg 1995). Differential
619 gene expression was performed at 5 DAP and 10 DAP for the following comparisons: Midas
620 *versus* G12873, AD *versus* AW; AD_Snap *versus* AD; AD_Snap *versus* AW; and MD *versus*
621 MW.

622

623 ***qRT-PCR of candidate genes for the qPD5.1-Pv locus***

624 The indehiscent variety Midas and three parental lines of the IL mapping population with the
625 highest level of pod shattering (ILs 232B, 244A/1A, 038B/2A2), and that were near isogenic to
626 Midas after three backcrosses, were grown in a greenhouse at the Max Planck Institute of
627 Molecular Plant Physiology (Golm-Potsdam, Germany), in April to July 2018. The plants were
628 individually grown in pots (diameter, 20 cm; volume, 3 L), and fertilisation was performed with
629 Hakaphos rot (0.015%) during irrigation (666 g/10 L). The plants were watered four times per
630 day, and pest control was performed using Neem Azal (6 mL/3 L). At least nine biological
631 replicates were grown for each genotype. At least three pods from each dehiscent genotype and
632 four pods for Midas were collected from different replicates, at 2, 3, 4, 5, 7, 9, 11 and 13 DAP.
633 Entire green pods were collected from 2 DAP to 5 DAP, while from 7 DAP, the ventral and
634 dorsal sutures were separated manually from the valves and collected separately to evaluate gene
635 expression in the region surrounding the ventral suture. The pods were frozen in liquid nitrogen
636 before storage at -80 °C. The pod tissues were ground with a mixer mill (MM400; Retsch), and
637 the RNA was extracted using the RNA miniprep kit (Direct-zol; Zymo Research GmbH). The

638 RNA was stained using GelRed, and its integrity was visualised using 1% agarose gels. The RNA
639 concentrations and quality were measured using a spectrophotometer (NanoDrop OneC; Thermo
640 Scientific). After adjusting the RNA concentrations, the cDNA was synthesized for each sample
641 (Maxima First Strand cDNA Synthesis Kit with dsDNase; Thermo Scientific). Each cDNA was
642 diluted 1:10, by adding HPLC quality water, and stored at -80 °C. The primers for the candidate
643 genes (i.e., qRT-PCR) were designed based on the gene coding sequences using the Primer3
644 (v0.4.0) tool (Supplemental Table 9). The target candidate genes were selected based on gene
645 annotation, gene expression from the RNA-seq data, the presence of selection signatures
646 according to Schmutz *et al.* (2014) and Bellucci *et al.* (2014), the functions of orthologous genes,
647 and the location in the genomic regions with high association to pod shattering. Two
648 housekeeping genes were included, based on the literature (i.e., Phvul.007G270100 (Borges *et*
649 *al.*, 2012); Phvul.010G122200 (Montero-Tavera *et al.*, 2017). The amplification efficiencies were
650 determined for each pair of primers. Here, four dilutions (i.e., 1:10, 1:20, 1:30, 1:40) of the same
651 cDNA were amplified (i.e., qRT-PCR), and the slope (R^2) of the calibration curve was used to
652 infer the primer efficiency, according to Equation (1):

653

$$654 \quad \text{Efficiency (\%)} = (E - 1) \times 100 \quad (1),$$

655

656 where E was obtained from R^2 according to the Equation (2):

657

$$658 \quad E = 10^{-1/\text{slope}} \quad (2).$$

659

660 The differential gene expression was calculated as fold-changes between each dehiscent
661 line (i.e., 232B, 244A/1A, 038B/2A2) and the indehiscent line Midas, and for all of the donor
662 parents grouped together *versus* Midas, according to Schmittgen and Livak (2008). T-tests were
663 performed for each comparison separately, as comparisons of the ΔCt values. ΔCt was obtained
664 as the difference between the Ct (cycle threshold) of the candidate gene and the Ct of the
665 housekeeping gene for normalisation of gene expression, according to Schmittgen and Livak
666 (2008).

667

668 ***Identification of orthologous genes with putative functions in pod shattering***

669 The common bean genome (v2.1) (<http://phytozome.jgi.doe.gov/>) contains 27,433 loci and
670 36,995 protein-coding transcripts. However, for several of these, the annotation is missing or not
671 always accurate. We used the Orthofinder algorithm (Emms and Kelly 2015) to identify clusters
672 of orthologous genes among the proteome of *P. vulgaris*, nine related legume species and *A.*
673 *thaliana*. The proteome sequences considered here were: *A. thaliana* (TAIR10); *P. vulgaris*
674 (v2.1); *G. max* (Wm82.a2.v1); *M. truncatula* (285_Mt4.0v1); *V. unguiculata* (v1.1); *Cicer*
675 *arietinum* (cicar.ICC4958.gnm2.ann1); *Lotus japonicus* (v3.0); *Lupinus angustifolius* (1.0);
676 *Vigna angularis* (vigan.Gyeongwon.gnm3.ann1.3Nz5); *Vigna radiata*
677 (vigra.VC1973A.gnm6.ann1); and *Glycyrrhiza uralensis* (Gur.draft-genome.20151208). These
678 were downloaded from: Phytozome (<http://phytozome.jgi.doe.gov/>); the ILS database
679 (<https://legumeinfo.org/>); the *Lotus japonicus* genome assembly (<http://www.kazusa.or.jp/lotus/>);
680 and the *Glycyrrhiza uralensis* genome database ([http://ngs-data-archive.psc.riken.jp/Gur-](http://ngs-data-archive.psc.riken.jp/Gur-genome/index.pl)
681 [genome/index.pl](http://ngs-data-archive.psc.riken.jp/Gur-genome/index.pl)). The protein sequences from the primary transcripts were used for the analysis,
682 except for *L. japonicus*, for which only the full proteome was available. Orthofinder (v2.1.2)
683 identified 20,692 orthogroups (i.e., clusters of orthologous genes) across these 11 species. The
684 list of structural genes involved in the synthesis of phenylpropanoid was obtained from the Plant
685 Metabolic Network database (<https://www.plantcyc.org/>) for common bean, soybean and *A.*
686 *thaliana*, as pod shattering in common bean is positively associated with lignin content in the
687 pods (Murgia *et al.*, 2017). Common bean genes without any clear annotation were considered as
688 putative structural genes of phenylpropanoid synthesis if they clustered in the same orthogroup of
689 *A. thaliana* and soybean lignin biosynthesis-related genes. *A. thaliana* and soybean lignin-related
690 genes that were not assigned to any orthogroup were blasted with BLASTp against the common
691 bean proteome to identify the best putative orthologues. Common bean gene orthologues to those
692 with a well-known role or a putative function in seed dispersal mechanisms in *A. thaliana* and in
693 other crops, according to the available literature, were also identified with the same approach.

694

695 ***Identification of selection signatures***

696 Genes that underwent selection during domestication of common bean in Mesoamerica and in the
697 Andes (Schmutz *et al.*, 2014) were identified. Moreover, 27,243 contigs that were previously
698 detected by Bellucci *et al.* (2014), which included 2,364 putatively under selection in the
699 Mesoamerican pool, were mapped against the last common bean genome version. Briefly, the
700 contigs were aligned against the *P. vulgaris* protein sequences of all of the gene coding sequences
701 (annotation on Phytozome, version 2.1) using NCBI blastx (blast-2.2.26), and then the best hit for
702 each contig was selected and the reference gene of each contig was established with a threshold
703 of $<1 \text{ E-}10$. A gene was considered as putatively under selection if at least one of the five contigs
704 with the best e values was putatively under selection in Bellucci *et al.* (2014).

705

706 ***Pod histological analysis on parental lines of the IL population***

707 Pods of the highly shattering genotypes 232B, 244A/1A and 038B/2A2 (ILs) and the totally
708 indehiscent variety Midas were collected for histological investigation. These were from the same
709 greenhouse experiment that was performed for the qRT-PCR expression analysis. In addition,
710 replicates of genotype MG38 (RIL) were grown in the same experiment. Entire pods were
711 collected across five developmental stages (6, 10, 14, 18, 30 DAP). Then 2-cm to 3-cm free-hand
712 cross sections from the pods were fixed in 5% agarose, and 70 μm , 50 μm and 30 μm cross-
713 sections were obtained using a microtome (VT 1000 S; Leica). A solution of phloroglucinol (7
714 mg), methanol (7 mL) and 37% chloridric acid (7 mL) was applied to the pod sections for
715 specific lignin staining. The pod sections were visualised under an optical microscope (BX51TF;
716 Olympus).

717

718 **Supplemental Data**

719 **Supplemental Figure 1.** Analysis of lignification patterns in the dorsal sheaths of 6-day-old pods
720 of the totally indehiscent variety Midas (A, B) and the highly pod shattering IL 244A/1A (C, D).

721 **Supplemental Figure 2.** Analysis of lignification patterns in pod valves of 10-day-old pods of
722 the totally indehiscent variety Midas (A), and of two highly pod shattering RIL MG38 (B) and IL
723 244A/1A(C).

724 **Supplemental Figure 3.** Analysis of lignification patterns in the ventral sheaths of 14-day-old
725 pods of the totally indehiscent variety Midas (A, B) and the highly pod shattering RIL MG38 (C,
726 D) and IL 244A/1A (E, F).

727 **Supplemental Figure 4.** Densities of the 19,420 SNP markers identified within a 1-Mb window
728 size using genotyping by sequencing.

729 **Supplemental Figure 5.** Genome-wide association study for occurrence of pod shattering on the
730 IL population.

731 **Supplemental Figure 6.** Expanded major QTL for pod shattering on chromosome Pv05.

732 **Supplemental Figure 7.** Physical positions of the putative structural genes for lignin
733 biosynthesis on the common bean chromosomes.

734 **Supplemental Figure 8.** Gene expression by qRT-PCR for Phvul.005G157600 for the pods of
735 the three highly dehiscent ILs (as indicated, blue) and for the indehiscent pods of variety Midas
736 (MIDAS, red) across the eight developmental stages from 2 DAP to 13 DAP.

737 **Supplemental Figure 9.** Schematic representation of the development of the BC4/F4
738 introgression line population.

739 **Supplemental Figure 10.** Structure of the GBS library.

740 **Supplemental Table 1.** Segregation of pod shattering on a subset of the BC4/F2 lines.

741 **Supplemental Table 2.** Observed segregation for the trait of ‘pod shattering occurrence’ in the
742 BC4/F2 population, and for each subpopulation.

743 **Supplemental Table 3.** Results of the post-harvest phenotyping for pod shattering for 549
744 BC4/F3 IIs.

745 **Supplemental Table 4.** Results of field and post-harvest phenotyping for pod shattering for
746 1,197 BC4/F4 IIs.

747 **Supplemental Table 5.** Summary of the genome-wide association study for pod shattering in the
748 BC/F4 IIs population.

749 **Supplemental Table 6.** Differential gene expression by qRT-PCR of the target candidate genes
750 at the major locus *qPD5.1-Pv* for pod indehiscence.

751 **Supplemental Table 7.** Summary of the best candidate genes at the major locus *qPD5.1-Pv*,
752 according to the expression data (i.e., RNA-seq, qRT-PCR), the presence of a selection signature
753 (Schmutz *et al.* (2014) and Bellucci *et al.* [20]), and gene annotation of the common bean gene
754 and its orthologues in *A. thaliana* and other crops.

755 **Supplemental Table 8.** Post-harvest phenotyping for the scoring of pod shattering of the IL
756 population.

757 **Supplemental Table 9.** Primers sequences for qRT-PCR and gene expression analysis of the
758 target candidate genes at the major locus *qPD5.1-Pv* for pod indehiscence.

759 **Supplemental Table 10.** Sequences of the single-stranded oligos for the adapters used for GBS
760 library preparation.

761 **Supplemental Table 11.** Sequences of the primers used for the amplification, indexing and
762 quantification of the GBS library.

763 **Supplemental Data Set 1.** Genes identified within the major locus *qPD5.1-Pv* for loss of pod
764 shattering.

765 **Supplemental Data Set 2.** Genes in common bean that are orthologous to genes in other species
766 with known functions that are putatively involved in seed shattering or have potentially related
767 functions (e.g., cell-wall modification, differentiation).

768 **Supplemental Data Set 3.** Genes in common bean that are putatively involved in the
769 phenylpropanoid biosynthesis pathway.

770 **Supplemental Data Set 4.** List of accessions that were grown for pod collection, RNA-seq and
771 differential gene expression analyses.

772 **SUPPLEMENTAL METHODS.** *GBS library preparation*

773 **SUPPLEMENTAL REFERENCES**

774

775

776 **Acknowledgments**

777 The study was part of the PhD research work of the first author (V.D) and he is grateful to the
778 Doctoral School of the Polytechnic University of Marche (UNIVPM) and to the
779 FORSCHUNGSZENTRUM JÜLICH (IBG-2) that co-funded the PhD scholarship.

780 This work was supported by the BRESOV project, funded from the European Union's Horizon
781 2020 research and innovation program under Grant Agreement No. 774244, the Italian
782 Government (MIUR; Grant number RBFR13IDFM_001, FIRB Project 2013), and the
783 Polytechnic University of Marche.

784 Alisdair R. Fernie and Saleh Alseekh acknowledge the European Union project PlantaSyst (SGA-
785 CSA No 664621 and No 739582 under FPA No. 664620).

786 We are grateful to Prof. Paul Gepts for providing the MG38 genotype, which was used as a donor
787 parental line for the development of the population in the earlier stage of the research, and to the
788 Sequentia Biotech for the bioinformatic analyses on RNA-seq data.

789 Valerio Di Vittori is grateful to Dr Leonardo Perez de Souza, José G. Vallarino and Federico
790 Scossa for their help and critical input in the differential gene expression analysis and
791 identification of orthologous genes.

792

793

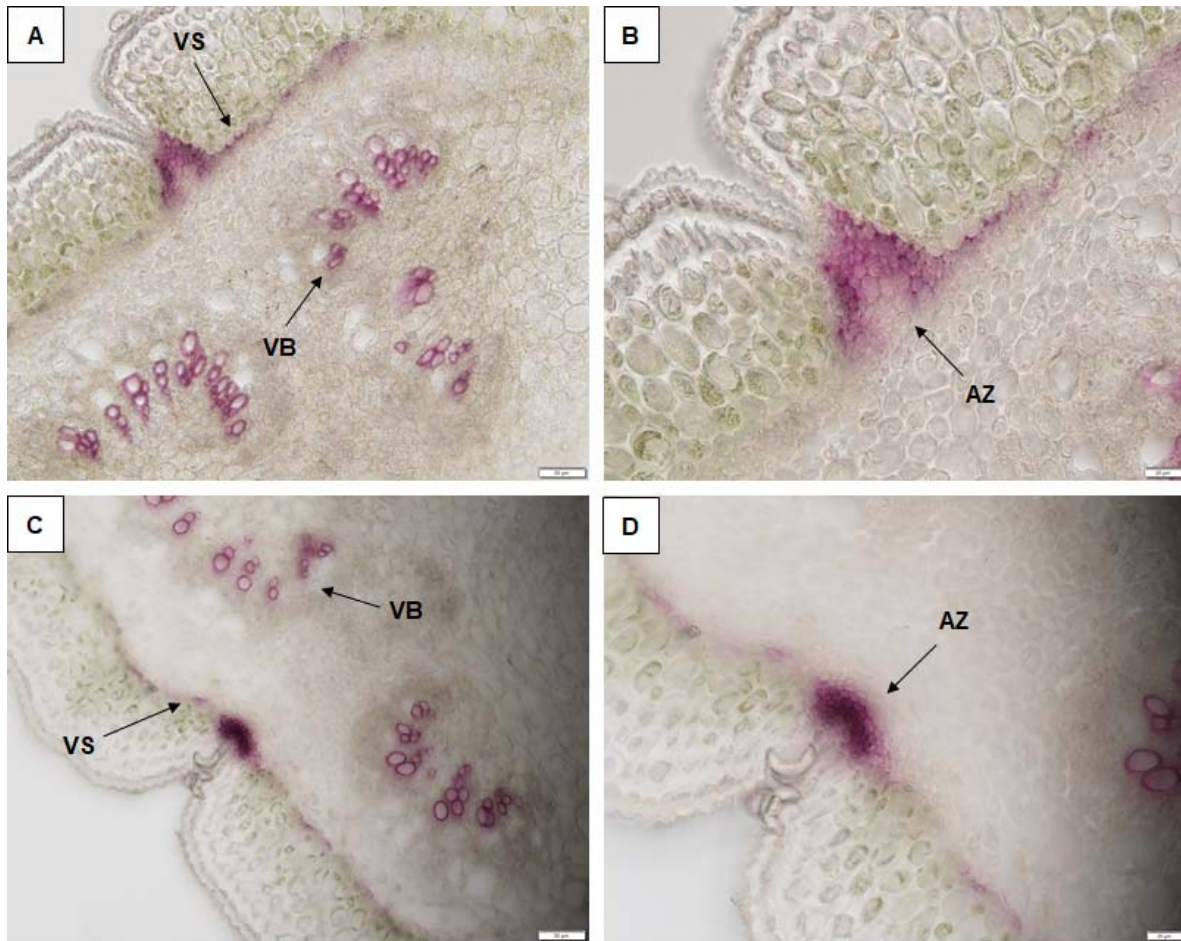
794 **Author Contributions**

795 **R.P** conceived and supervised the study; **V.D** and **R.P** designed the study and wrote the article;
796 **V.D, E.Bi, E.Be, L.N, D.R, M.Rod, GA, J.F, A.C, G.L, S.M** and **R.P** contributed in the
797 development of the IL population; **V.D, T.G, M.L.M, F.F and B.U** were involved in the
798 phenotyping; **V.D, M.Ros, C.D, M.D and C.X** were involved in genotyping and bioinformatic
799 analyses; **M.Rod** performed GWAS; **E.B** provided the RNA-seq data; **V.D.** performed the qRT-
800 PCR experiment, the differential expression analysis, the histological analysis and orthologue
801 identification under the supervision of **S.A** and **A.R.F** and with critical input from **A.S** and **A.F**.
802 All of the authors have read and approved the final version of the manuscript, with further critical
803 input.

804

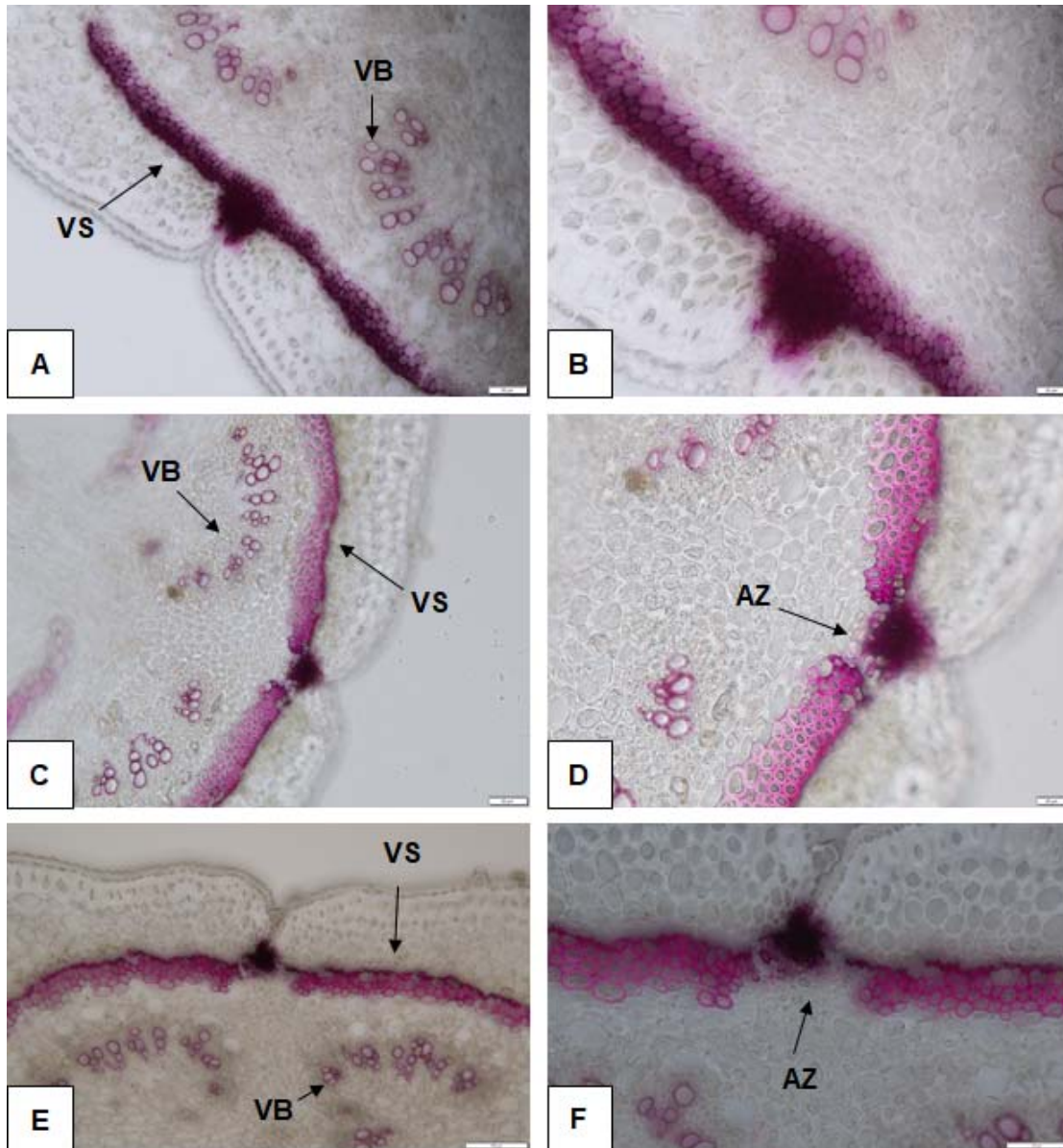
805

806 **FIGURES**



807
808 **Figure 1. Analysis of lignification patterns in the ventral sheaths of 6-day-old pods of the totally**
809 **indehiscent variety Midas (A, B) and the highly dehiscent IL 244A/1A (C, D). Cross-sections (section**
810 **thickness, 30 μm) of pods after phloroglucinol staining for lignin. (B, D) Increased magnification from (A,**
811 **C). Scale bars: 50 μm (A, C); 20 μm (B, D). VS, ventral sheath; VB, vascular bundles; AZ, abscission**
812 **zone.**
813

814



815

816 **Figure 2. Analysis of lignification patterns in the ventral sheaths of 10-day-old pods of the totally**

817 **indehiscent variety Midas (A, B) and the highly dehiscent RIL MG38 (C, D) and IL 244A/1A (E, F).**

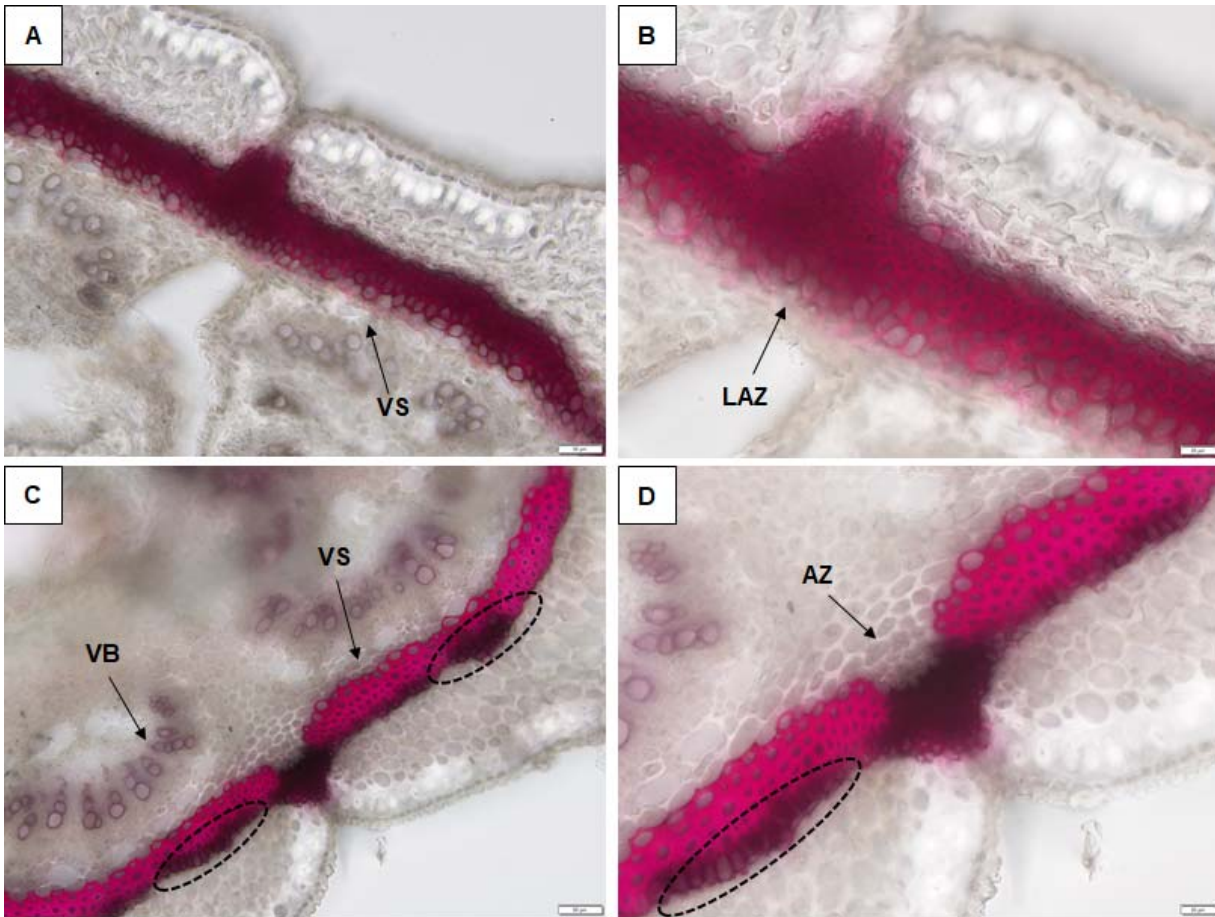
818 Cross-sections (section thickness, 30 μm) of pods after phloroglucinol staining for lignin. (B, D, F)

819 Increased magnification from (A, C, E). Scale bars: 50 μm (A, C, F); 20 μm (B, D); 100 μm (E). VS,

820 ventral sheath; VB, vascular bundles; AZ, abscission zone.

821

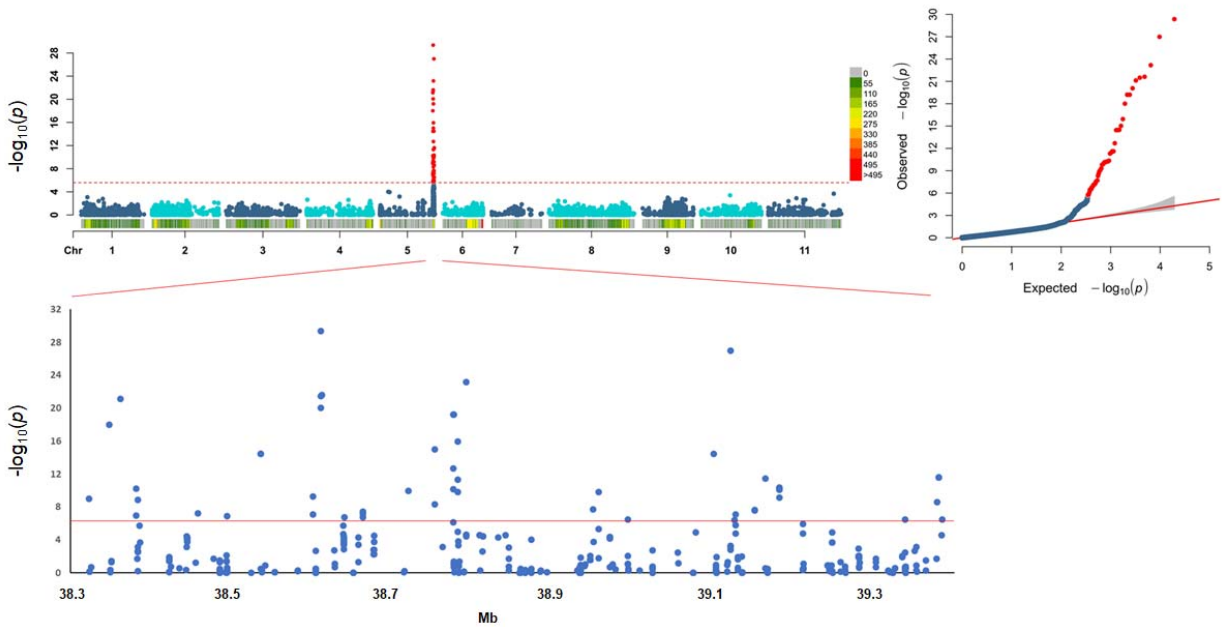
822



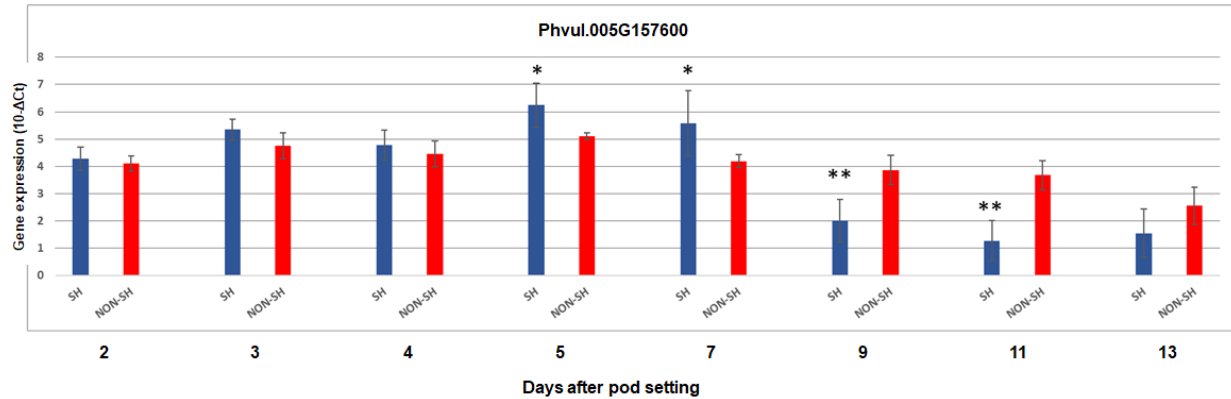
823
824 **Figure 3. Analysis of lignification patterns of the ventral sheaths in 30-day-old pods (i.e., mature**
825 **pods) of the totally indehiscent variety Midas (A, B) and the highly dehiscent IL 038A/2A2 (C, D).**
826 **Cross-sections (section thickness, 50 μm) of the ventral suture after phloroglucinol staining for lignin. (B,**
827 **D) Increased magnification from (A, C). Scale bars: 50 μm (A, C); 20 μm (B, D). VS, ventral sheath; VB,**
828 **vascular bundles; AZ, abscission zone; LAZ, lignified abscission zone. (C, D) Dotted ellipses,**
829 **lignification areas with no strong cell wall thickening along the ventral sheath.**

830

831



832 **Figure 4. Genome-wide association study for occurrence of pod shattering.** Top left: Manhattan plot
833 to show the associations between 52 SNP markers (red dots on distal region of chromosome Pv05) and the
834 SH y/n trait (dehiscent vs indehiscent lines). Dashed red line, fixed threshold of significance for the 19,420
835 SNP markers physically distributed across the 11 common bean chromosomes. Top right: QQplot of the
836 distribution of the observed p values compared to the expected distribution. Bottom: Expanded major QTL
837 on the distal part of chromosome Pv05, defining the significance of the SNP markers from 38.3 to 39.4
838 Mb on chromosome Pv05.
839



840

841 **Figure 5. Gene expression by qRT-PCR for Phvul.005G157600 for the pods of the combined three**
842 **highly dehiscent lines (SH; blue) and for the indehiscent pods of variety Midas (NON-SH; red)**
843 **across the eight developmental stages from 2 DAP to 13 DAP. The mean pod expression for the three**
844 **highly dehiscent introgression lines (038B/2A2, 244A/1A, 232B) is shown. *, p <0.05; **, p <0.01; SH**
845 **versus NON-SH. Data are means ±standard deviation of the biological replicates (n = 3 for each highly**
846 **dehiscent line for a total of nine for SH; n=4 for NON-SH). T.test for detection of significant differences,**
847 **homoscedastic, two tails.**

848

849

850

Parsed Citations

Bellucci, E. et al. (2014). Decreased nucleotide and expression diversity and modified co-expression patterns characterize domestication in the common bean. *Plant Cell* 26, 1901–1912.

Pubmed: [Author and Title](#)

Google Scholar: [Author Only Title Only Author and Title](#)

Benjamini, Y. and Hochberg, Y. (1995). Controlling the false discovery rate: a practical and powerful approach to multiple testing. *J. R. Statist.* 57, 289–300.

Pubmed: [Author and Title](#)

Google Scholar: [Author Only Title Only Author and Title](#)

Bitocchi, E. et al. (2017). Beans (*Phaseolus* spp.) as a model for understanding crop evolution. *Front. Plant Sci.* 8, 722.

Pubmed: [Author and Title](#)

Google Scholar: [Author Only Title Only Author and Title](#)

Bitocchi, E. et al. (2013). Molecular analysis of the parallel domestication of the common bean (*Phaseolus vulgaris*) in Mesoamerica and the Andes. *New Phytol.* 197, 300–313.

Pubmed: [Author and Title](#)

Google Scholar: [Author Only Title Only Author and Title](#)

Borges, A., Tsai, S.M. and Caldas, D.G. (2012). Validation of reference genes for RT-qPCR normalization in common bean during biotic and abiotic stresses. *Plant Cell Rep.* 31, 827–838.

Pubmed: [Author and Title](#)

Google Scholar: [Author Only Title Only Author and Title](#)

Boycheva, S., Daviet, L., Wolfender, J. and Fitzpatrick, T.B. (2014). The rise of operon-like gene clusters in plants. *Trends Plant Sci.* 19, 447–459.

Pubmed: [Author and Title](#)

Google Scholar: [Author Only Title Only Author and Title](#)

Browning, B. L., Zhou, Y. and Browning, S. R. (2018). A one-penny imputed genome from next-generation reference panels. *Am. J. Hum. Genet.* 103, 338–348.

Pubmed: [Author and Title](#)

Google Scholar: [Author Only Title Only Author and Title](#)

Bryan, A.C., Obaidi, A., Wierzba, M. and Tax, F.E. (2011). XYLEM INTERMIXED WITH PHLOEM1, a leucine-rich repeat receptor-like kinase required for stem growth and vascular development in *Arabidopsis thaliana*. *Planta* 235, 111–122.

Pubmed: [Author and Title](#)

Google Scholar: [Author Only Title Only Author and Title](#)

Di Vittori, V. et al. (2019) Convergent evolution of the seed-shattering trait. *Genes* 10, 68.

Pubmed: [Author and Title](#)

Google Scholar: [Author Only Title Only Author and Title](#)

Dong, Y. et al. (2014). Pod dehiscence resistance associated with domestication is mediated by a NAC gene in soybean. *Nat. Commun.* 5, 3352.

Pubmed: [Author and Title](#)

Google Scholar: [Author Only Title Only Author and Title](#)

Elshire, R.J. et al. (2011). A robust, simple genotyping-by-sequencing (GBS) approach for high diversity species. *PLoS ONE* 6 (5), e19379.

Pubmed: [Author and Title](#)

Google Scholar: [Author Only Title Only Author and Title](#)

Emms, D.M. and Kelly, S. (2015). OrthoFinder: solving fundamental biases in whole genome comparisons dramatically improves orthogroup inference accuracy. *Genome Biol.* 16, 157.

Pubmed: [Author and Title](#)

Google Scholar: [Author Only Title Only Author and Title](#)

Fourquin, C. et al. (2013). A change in SHATTERPROOF protein lies at the origin of a fruit morphological novelty and a new strategy for seed dispersal in *Medicago* genus. *Plant Physiol.* 162, 907–917.

Pubmed: [Author and Title](#)

Google Scholar: [Author Only Title Only Author and Title](#)

Funatsuki, H. et al. (2014). Molecular basis of a shattering resistance boosting global dissemination of soybean. *Proc. Natl. Acad. Sci. U.S.A.* 111, 17797–17802.

Pubmed: [Author and Title](#)

Google Scholar: [Author Only Title Only Author and Title](#)

Gepts, P. and Debouck, D.G. (1991). Origin, domestication, and evolution of the common bean (*Phaseolus vulgaris* L.). In *Common Beans: Research for Crop Improvement*; Voysest, O., Van Schoonhoven, A., Eds.; CAB: Oxon, UK 7–53.

Pubmed: [Author and Title](#)

Google Scholar: [Author Only Title Only Author and Title](#)

- Gioia, T., Logozzo, G., Kami, J., Spagnoletti Zeuli, P. and Gepts, P. (2013).** Identification and characterization of a homologue to the *Arabidopsis* INDEHISCENT gene in common bean. *J. Hered.* **104**, 273–286.
Pubmed: [Author and Title](#)
Google Scholar: [Author Only](#) [Title Only](#) [Author and Title](#)
- Gu, Q., Ferrándiz, C., Yanofsky, M.F. and Martienssen, R. (1998)** The FRUITFULL MADS-box gene mediates cell differentiation during *Arabidopsis* fruit development. *Development* **125**, 1509–1517.
Pubmed: [Author and Title](#)
Google Scholar: [Author Only](#) [Title Only](#) [Author and Title](#)
- Hammer, K. (1984).** Das Domestikationssyndrom. Die Kulturpflanze. **32**, 11–34.
Pubmed: [Author and Title](#)
Google Scholar: [Author Only](#) [Title Only](#) [Author and Title](#)
- Hofhuis, H. et al. (2016).** Morphomechanical innovation drives explosive seed dispersal. *Cell* **166**, 222–233.
Pubmed: [Author and Title](#)
Google Scholar: [Author Only](#) [Title Only](#) [Author and Title](#)
- Jinn, T.L., Stone, J.M. and Walker, J.C. (2000).** HAESA, an *Arabidopsis* leucine-rich repeat receptor kinase, controls floral organ abscission. *Genes Dev.* **14**, 108–117.
Pubmed: [Author and Title](#)
Google Scholar: [Author Only](#) [Title Only](#) [Author and Title](#)
- Koinange, E.M.S., Singh, S.P. and Gepts, P. (1996).** Genetic control of the domestication syndrome in common bean. *Crop Sci.* **36**, 1037–1045.
Pubmed: [Author and Title](#)
Google Scholar: [Author Only](#) [Title Only](#) [Author and Title](#)
- Konishi, S. et al. (2006).** An SNP caused loss of seed shattering during rice domestication. *Science* **312**, 1392–1396.
Pubmed: [Author and Title](#)
Google Scholar: [Author Only](#) [Title Only](#) [Author and Title](#)
- Lamprecht, H. (1932).** Beiträge zur Genetik von *Phaseolus vulgaris*. *Hereditas* **16**, 169–211.
Pubmed: [Author and Title](#)
Google Scholar: [Author Only](#) [Title Only](#) [Author and Title](#)
- Li, H. and Durbin, R. (2009).** Fast and accurate short read alignment with Burrows-Wheeler transform. *Bioinformatics* **25**, 1754–1760.
Pubmed: [Author and Title](#)
Google Scholar: [Author Only](#) [Title Only](#) [Author and Title](#)
- Liljegren, S.J. et al. (2004).** Control of fruit patterning in *Arabidopsis* by INDEHISCENT. *Cell* **116**, 843–853.
Pubmed: [Author and Title](#)
Google Scholar: [Author Only](#) [Title Only](#) [Author and Title](#)
- Liljegren, S.J. et al. (2000).** SHATTERPROOF MADS-box genes control seed dispersal in *Arabidopsis*. *Nature* **404**, 766–770.
Pubmed: [Author and Title](#)
Google Scholar: [Author Only](#) [Title Only](#) [Author and Title](#)
- Lo, S. et al. (2018).** Identification of QTL controlling domestication-related traits in cowpea (*Vigna unguiculata* L. Walp). *Sci. Rep.* **8**, 6261.
Pubmed: [Author and Title](#)
Google Scholar: [Author Only](#) [Title Only](#) [Author and Title](#)
- Love, M., Huber, W. and Anders, S. (2014).** Moderated estimation of fold change and dispersion for RNA-seq data with DESeq2. *Genome Biol.* **15**, 550.
Pubmed: [Author and Title](#)
Google Scholar: [Author Only](#) [Title Only](#) [Author and Title](#)
- Martin, M. (2011).** Cutadapt removes adapter sequences from high-throughput sequencing reads. *EMBnet.journal* **17**, 10–12.
doi.org/10.14806/ej.17.1.200.
Pubmed: [Author and Title](#)
Google Scholar: [Author Only](#) [Title Only](#) [Author and Title](#)
- McKenna, A. et al. (2010).** The Genome Analysis Toolkit: a MapReduce framework for analyzing next-generation DNA sequencing data. *Genome Res.* **20**, 1297–1303.
Pubmed: [Author and Title](#)
Google Scholar: [Author Only](#) [Title Only](#) [Author and Title](#)
- Mitsuda, N. and Ohme-Takagi, M. (2008).** NAC transcription factors NST1 and NST3 regulate pod dehiscence in a partially redundant manner by promoting secondary wall formation after the establishment of tissue identity. *Plant J.* **56**, 768–778.
Pubmed: [Author and Title](#)
Google Scholar: [Author Only](#) [Title Only](#) [Author and Title](#)
- Montero-Tavera, V., Escobedo-Landín, M.A., Acosta-Gallegos, J.A., Anaya-Lopez, J.L. and Ruiz-Nieto, J.E. (2017).** 26S: Novel reference

gene from leaves and roots of common bean for biotic stress expression studies based on PCR. *Legume Research* 40, 429–433.

Pubmed: [Author and Title](#)

Google Scholar: [Author Only Title Only Author and Title](#)

Murgia, M.L. et al. (2017). A comprehensive phenotypic investigation of the "pod-shattering syndrome" in common bean. *Front. Plant Sci.* 8, 251.

Pubmed: [Author and Title](#)

Google Scholar: [Author Only Title Only Author and Title](#)

Nanni, L. et al. (2011). Nucleotide diversity of a genomic sequence similar to SHATTERPROOF (PvSHP1) in domesticated and wild common bean (*Phaseolus vulgaris* L.). *Theor. Appl. Genet.* 123, 1341–1357.

Pubmed: [Author and Title](#)

Google Scholar: [Author Only Title Only Author and Title](#)

Osbourn, A. (2010). Gene clusters for secondary metabolic pathways: an emerging theme in plant biology. *Plant Physiol.* 154, 531–535.

Pubmed: [Author and Title](#)

Google Scholar: [Author Only Title Only Author and Title](#)

Parker, T.A., Berny Mier y Teran, J.C., Palkovic, A., Jernstedt, J. and Gepts, P. (2020). Pod indehiscence is a domestication and aridity resilience trait in common bean. *New Phytol.* 225, 558–570.

Pubmed: [Author and Title](#)

Google Scholar: [Author Only Title Only Author and Title](#)

R Core Team. (2019). The R project for statistical computing. www.R-project.org/.

Pubmed: [Author and Title](#)

Google Scholar: [Author Only Title Only Author and Title](#)

Rau, D. et al. (2019). Genomic dissection of pod shattering in common bean: mutations at non-orthologous loci at the basis of convergent phenotypic evolution under domestication of leguminous species. *Plant J.* 97, 693–714.

Pubmed: [Author and Title](#)

Google Scholar: [Author Only Title Only Author and Title](#)

Schmittgen, T. and Livak, K. (2008). Analyzing real-time PCR data by the comparative CT method. *Nat. Protoc.* 3, 1101–1108.

Pubmed: [Author and Title](#)

Google Scholar: [Author Only Title Only Author and Title](#)

Schmutz, J. et al. (2014). A reference genome for common bean and genome-wide analysis of dual domestications. *Nat. Genet.* 46, 707–713.

Pubmed: [Author and Title](#)

Google Scholar: [Author Only Title Only Author and Title](#)

Takahashi, Y. et al. (2019a). Domesticating *Vigna stipulacea*: a potential legume crop with broad resistance to biotic stresses. *Front. Plant Sci.* 10, 1607.

Pubmed: [Author and Title](#)

Google Scholar: [Author Only Title Only Author and Title](#)

Takahashi, Y. et al. (2019b). Genetic factor for twisting legume pods identified by fine-mapping of shattering-related traits in azuki bean and yard-long bean. [bioRxiv doi.org/10.1101/774844](https://doi.org/10.1101/774844).

Pubmed: [Author and Title](#)

Google Scholar: [Author Only Title Only Author and Title](#)

Van der Does, D. et al. (2017). The *Arabidopsis* leucine-rich repeat receptor kinase MIK2/LRR-KISS connects cell wall integrity sensing, root growth and response to abiotic and biotic stresses. *PLoS Genet.* 13, e1006832.

Pubmed: [Author and Title](#)

Google Scholar: [Author Only Title Only Author and Title](#)

Vasova, A. et al. (2016). Genome and transcriptome analysis of the Mesoamerican common bean and the role of gene duplications in establishing tissue and temporal specialization of genes. *Genome Biol.* 17, 32.

Pubmed: [Author and Title](#)

Google Scholar: [Author Only Title Only Author and Title](#)

Vrebalov, J. et al. (2009). Fleshy fruit expansion and ripening are regulated by the tomato SHATTERPROOF gene TAGL1. *Plant Cell* 21, 3041–3062.

Pubmed: [Author and Title](#)

Google Scholar: [Author Only Title Only Author and Title](#)

Wallace, L., Arkwazee, H., Vining, K. and Myers, J.R. (2018). Genetic diversity within snap beans and their relation to dry beans. *Genes* 9, 587.

Pubmed: [Author and Title](#)

Google Scholar: [Author Only Title Only Author and Title](#)

Xu, S.L., Rahman, A., Baskin, T.I. and Kieber J.J. (2008). Two leucine-rich repeat receptor kinases mediate signaling, linking cell-wall biosynthesis and ACC synthase in *Arabidopsis*. *Plant Cell* 20, 3065–3079.

Pubmed: [Author and Title](#)

Google Scholar: [Author Only Title Only Author and Title](#)

Yang, C. et al. (2007). Arabidopsis MYB26/MALE STERILE35 regulates secondary thickening in the endothecium and is essential for anther dehiscence. Plant Cell 19, 534–548.

Pubmed: [Author and Title](#)

Google Scholar: [Author Only](#) [Title Only](#) [Author and Title](#)

Yang, C. et al. (2017). Transcription factor MYB26 is key to spatial specificity in anther secondary thickening formation. Plant Physiol. 175, 333–350.

Pubmed: [Author and Title](#)

Google Scholar: [Author Only](#) [Title Only](#) [Author and Title](#)

Yoon, J. et al. (2014). The BEL1 type homeobox gene SH5 induces seed shattering by enhancing abscission-zone development and inhibiting lignin biosynthesis. Plant J. 79, 717–728.

Pubmed: [Author and Title](#)

Google Scholar: [Author Only](#) [Title Only](#) [Author and Title](#)

Zhang, J., Xie, M., Tuskan, G.A, Muchero, W. and Chen, J-G. (2018). Recent advances in the transcriptional regulation of secondary cell-wall biosynthesis in the woody plants. Front. Plant Sci. 9, 1535.

Pubmed: [Author and Title](#)

Google Scholar: [Author Only](#) [Title Only](#) [Author and Title](#)

Zhong, R., Lee, C., Zhou, J., McCarthy, R.L. and Ye, Z-H. (2008). A battery of transcription factors involved in the regulation of secondary cell-wall biosynthesis in Arabidopsis. Plant Cell 20, 2763–2782.

Pubmed: [Author and Title](#)

Google Scholar: [Author Only](#) [Title Only](#) [Author and Title](#)